Curved detonation fronts in solid explosives: collisions and boundary interactions

J. B. Bdzil
Los Alamos National Laboratory
Los Alamos, NM 87545 USA

T. D. Aslam and D. S. Stewart
TAM Department, University of Illinois
Urbana, IL 61801 USA

Abstract: Detonation Shock Dynamics (DSD) can be used to model the effects that shock curvature κ has on detonation speed $D_n(\kappa)$. At the edges of the explosive, $D_n(\kappa)$ is supplemented with boundary conditons. By direct numerical simulation (DNS), we study how the reaction zone interacts with the edge. DSD theory has been integrated with the level-set method of Osher & Sethian and the Los Alamos DNS code Mesa to create a powerful tool for simulating complex explosive-containing systems.

Key words: Detonation, Curvature effect, Edge interactions, Mach reflection

1. Introduction

To accurately predict the propagation of detonation through an explosive, one needs to model the physics that occurs on the chemical reaction-zone scale η_r. In sharp contrast to the structured shocks observed for gaseous detonation, those for heterogeneous solid explosives are broadly curved on the η_r scale. The speed of the detonation is strongly influenced by the curvature of the shock κ; with reductions of speed of 40% in strongly divergent flows.

Safety concerns have led to the use of explosives that satisfy $\mathcal{L}/\eta_r = O(10^3)$, where $\mathcal{L}$ is a representative dimension of the explosive. Curvature effects have a strong influence on detonation in these systems, and highly resolved multidimensional simulations are "expensive." A body of theory and supporting experiments, called Detonation Shock Dynamics (DSD) (Bdzil & Stewart 1989), has been developed that treats these curvature effects (Aslam et al. 1995). The DSD front theory derives a speed function $D_n(\kappa)$ based on a weakly divergent, quasi-one-dimensional (1D) model of the detonation reaction zone. This function can also be determined directly from experiments. The regions of strongest flow divergence are found near the explosives' boundaries. Boundary conditions (BC) must be supplied in addition to $D_n(\kappa)$ to treat these interactions. The dynamics of broadly curved fronts, described by DSD, interacts with the edge

through a narrow boundary layer a few η_r thick, where the flow is both reactive and fully two dimensional (2D).

In Section 2 we give a brief review of DSD. Front theories require a front propagation algorithm. In Section 3 we describe an engineering implementation of DSD that uses a level-set (LS) algorithm (Osher & Sethian 1988) to propagate the DSD front (Aslam et al. 1995). To integrate DSD front theory with hydrodynamic simulations, an accurate method is needed to quickly burn the explosive and capture the detonation state consistent with $D_n(\kappa)$. In Section 4 we describe our new burn model and show a full DSD-based simulation. In Section 5 we discuss results obtained from high-resolution simulations of two edge problems: (1) the sudden loss of confinement, and (2) oblique interaction of detonation with a rigid wall. Owing to reaction-zone effects, we find that detonations exhibit von Neumann reflection (Colella & Henderson 1990).

2. DSD Theory

DSD is the name given to the body of multidimensional detonation theory and experiments that is used to describe the dynamics of detonation with broadly curved shocks on the reaction-zone scale η_r. The model equations used to describe this limit derive from the 2D, reactive Euler equations transformed to shock-attached, intrinsic coordinates. Shown in Fig. 1 is our coordinate net of straight lines normal and curves locally parallel to the shock, all moving with the shock normal speed D_n.

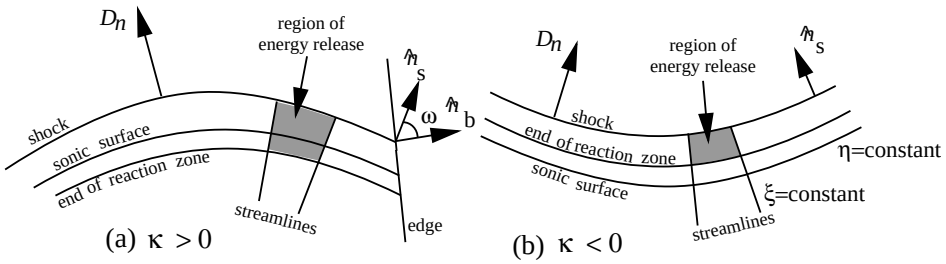

Figure 1. A snapshot showing the intrinsic coordinates and the definition of the boundary-edge angle ω; in (a) for a diverging detonation and in (b) for a converging detonation. The speed of the wave is influenced by two factors, the convergence/divergence and the location of the sonic surface.

2.1. Interior flow

The weak shock-curvature limit defined by $\kappa = O(\epsilon)$, where $\epsilon \equiv (reaction - zone\ scale)/(shock\ radius\ of\ curvature)$, is the basis of most theoretical analysis of 2D detonation. This limit envisions that $O(1)$ changes in the field vari-

ables occur over $O(\epsilon^{-1})$ distances in the ξ-direction, and the flow velocity in the ξ-direction is no greater than $O(\epsilon)$. Under these assumptions, the DSD-related time derivatives are $O(\epsilon)$, the flow is principally in the η-direction, and is "nozzle"-like (see Fig. 1), and 2D effects enters the flow only parametrically, via $\kappa(\xi, t)$. This limit allows for time dependence on the $O(1)$ reaction scale, provided no $O(1)$ velocities are generated in the ξ-direction. The various streamtubes then communicate with one another only through the shock-surface compatibility condition (i.e., through the LS equation or whichever propagation method we use). The DSD reaction zone equations are:

$$(\dot{\rho}) + \rho(D_n - U)_\eta = -\rho U \kappa \ , \tag{1}$$

$$\rho(\dot{U}) - P_\eta = 0 \ , \tag{2}$$

$$\rho^2(\dot{e}) - P(\dot{\rho}) = 0 \ , \tag{3}$$

where $(\dot{}) \equiv (\partial/\partial t)_{\eta,\xi} + (D_n - U)(\partial/\partial\eta)_{t,\xi}$ and ρ, U, P, $e(P, \rho, \lambda q)$, λ, and q are the density, laboratory particle velocity in the η- direction, pressure, specific internal energy, degree of reaction, and heat of detonation, respectively. Henceforth, when t, η, ξ, etc. are used as subscripts they denote partial derivatives. The *master equation*, derived from Eqs. (1–3) helps us analyze the 2D reaction zone

$$P_t + \rho(D_n - U)U_t = -\rho[(D_n - U)^2 - C^2]U_\eta + \sigma \ , \tag{4}$$

where $\sigma \equiv -(e_\lambda/e_P)R - \rho C^2 U\kappa$ and C, $-(e_\lambda/e_P)R \geq 0$, and $(\dot{\lambda}) \equiv R \geq 0$ are the sound speed, heat-release rate, and chemical rate law, respectively.

In its simplest realization, DSD theory assumes that $D_n/D_{CJ} = 1 + O(\epsilon)$, that the departures from the Zeldovich-von Neumann-Doring (ZND) limit are small, and neglects the inertia of the reaction zone (setting t derivatives in Eqs. (1–4) to zero). The reaction-zone structure is then obtained by solving the steady form of Eqs. (1–3), subject to the shock conditions and generalized Chapman-Jouguet (CJ) condition obtained from Eq. (4) (i.e., $(D_n - U)^2 - C^2 = 0$ when $\sigma = 0$, provided that $\kappa \geq 0$). This defines an eigenvalue problem that obtains $D_n(\kappa)$. Figure 1 shows that two effects contribute to $D_n \leq D_{CJ}$: (1) the divergence and (2) the movement of the sonic surface. For weakly convergent systems, effect (1) dominates and $D_n(\kappa) \geq D_{CJ}$ is derived by requiring $(D_n - U)^2 - C^2 = 0$ at the end of the reaction zone (i.e., $\lambda = 1$). Details can be found in (Bdzil 1981), (Bdzil & Stewart 1986), (Stewart et al. 1995), (Aslam et al. 1995) and references therin. Importantly for $D_n(\kappa)$, the shock evolves by parabolic dynamics and so is smooth. For real heterogeneous solid explosives, R is not well known. Then $D_n(\kappa)$ is determined directly from experiment. The $D_n(\kappa)$ for the explosive PBX 9502 is shown in Fig. 2a. Note the $O(1)$ variations of $(D_{CJ} - D_n)/D_{CJ}$.

2.2. Boundary conditions

The slow variations in the ξ-direction that are a part of DSD can break down at explosive boundaries. There the flow can be fully 2D and time-dependent on the $O(1)$ reaction-zone scale (Bdzil & Stewart 1986). On the slow-time DSD scale, this region can appear to be steady. Then the DSD and boundary regions are coupled as follows: (1) the DSD region drives the boundary with information on the shock slope and D_n, and in turn (2) the boundary region uses this data to return a (possibly) modified shock slope, etc. (Bdzil 1981). Using the boundary angle ω defined in Fig. 1, DSD supplies ω_{in} to the boundary flow, which then returns ω_{out} to the DSD region. The boundary is itself characterized by two angles that depend on the explosive/inert pair being considered: a critical angle ω_s and a confinement angle ω_c.

We've distilled these interactions into the following recipe. If $\omega_{in} < \omega_s$, then $\omega_{out} = \omega_{in}$; otherwise, $\omega_{out} = \omega_c$. The boundary dynamics are considered in more detail later in this paper.

3. Front propagators

Together, the $D_n(\kappa)$ function and the boundary conditions provide a complete dynamical description of the detonation front at the DSD level. A second element is needed to propagate the front: a shock compatibility condition that relates how changes in the speed of the front affect its shape. One of the most widely used forms of this condition is Whitham's ray method (Whitham 1973). Every section of the detonation front advances along a system of rays that resembles the bicharacteristic rays of geometrical optics. Although physically appealing, such methods can be logically complex. The front-attached rays converge and diverge with the front, which can lead to numerical problems. This is one member of the family of marker-particle or Lagrangian methods. Such methods are not well suited for engineering applications where the problem geometries are complex.

3.1. Level-set method

Osher and Sethian (1988) devised a powerful algorithm for propagating fronts with curvature-dependent speed. Their method obviates the need for the complex logic to treat collisions and avoids the problem of marker-particle methods. They consider the shock as a level curve $C(x, y, t) = 0$ embedded in a higher-dimensional LS function $\psi(x, y, t)$ that's defined on an Eulerian grid. The evolution equation for the LS function is derived by using the property $\psi(x, y, t) = constant$ along a level curve to obtain

$$\psi_t + \vec{D}_n(\kappa) \cdot \vec{\nabla}\psi = 0 \ . \tag{5}$$

Equation (5) is the LS-method surface compatibility condition.

The precise form selected for $\psi(x, y, 0)$ is unimportant, however, $\psi(x, y, 0)$ must be single valued. This insensitivity requires that; (1) D_n depend only on data from a single curve and (2) that the level curves not cross with time. The first property is automatic, since $D_n(\kappa)$. The second property follows from the fact that the distance between level curves, as measured by $d(x, y, t) = |\vec{\nabla}\psi(x, y, 0)|/|\vec{\nabla}\psi|$, does not go to zero. By way of example, for $D_n = D_{CJ} - \alpha\kappa$ with $\alpha \geq 0$, the d-equation (which is derived from Eq. 5) is

$$d_t + D_{CJ}\vec{n} \cdot \vec{\nabla}(d) = \alpha\kappa^2 d \ , \tag{6}$$

for a cylindrically symmetric system. Since $\alpha\kappa^2 \geq 0$ and $d(x, y, 0) = 1$, d increases with time. The result $d(x, y, t) > 0$ continues to hold for fully 2D systems with strong divergence at the boundaries (Aslam et al. 1995). In practice,

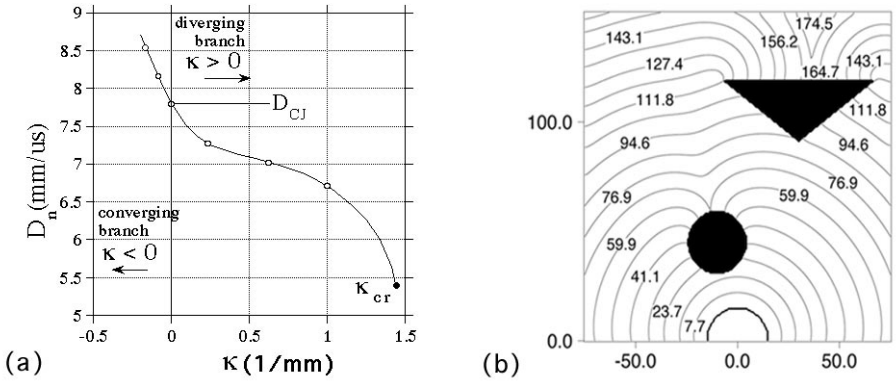

Figure 2. The $D_n(\kappa)$ for a typical condensed phase explosive, PBX 9502 is shown in Fig. 2a. Burn time contours for an engineering-style problem obtained with the LS-method are shown in Fig 2b. The dark areas are obstacles.

we assign $\psi = 0$ to the shock, with $\psi > 0$ in unburnt material and $\psi < 0$ in burnt material. The burn time $t_b(x, y)$ is taken as the first time that $\psi < 0$ at a point. Figure 2a shows the result of a LS calculation of the burn times for an engineering-style problem. Initially, the detonation is a semi-circle with origin (0,0) and obeys $D_n = 8$ mm/μs $- \kappa \times 66$ mm^2/μs everywhere. Bifurcation, merging, convergence, and divergence of the wave are all well captured. All of these ideas easily carryover to 3D.

4. Hydrodynamic simulations using DSD

The work that has gone into DSD was motivated by the need to capture reaction-zone effects in numerical simulations of engineering systems. Two elements are required to accomplish this goal: (1) accurate front evolution and (2)

an ability to deposit the proper detonation state (i.e., $P(D_n)$, $\rho(D_n)$, $U(D_n)$) at the front.

To address element (2), we've developed a numerical reaction-zone model that uses a "pseudo" divergence Ω in place of κ in simulations, so that a detonation state consistent with D_n is captured. To eliminate precursors to the $D_n(\kappa)$ wave, we built a model around the reaction zone equation of state (EOS), $e(P/\lambda, \rho, q)$, which together with the trigger provided by the DSD burn times $t_b(x, y)$, causes the numerical "reaction zone" to be on the weak detonation branch. Starting with $P = 0$ and $\lambda = 0$, at $t_b(x, y)$ the explosive is rapidly burned (i.e., $\lambda \to 1$ in about the time it takes the wave to traverse one computational zone). From Eq. (4) it follows that the ratio κ/R determines D_n. Since this nonphysical numerical reaction rate $\tilde{R}$ is associated with the size of the computational zones, we replace $U\kappa$ in Eqs. (3–4), by

$$U\kappa \Rightarrow \Omega\tilde{R} \ , \qquad R \Rightarrow \tilde{R} \ , \tag{7}$$

and then solve for $D_n(\Omega)$. Elimination then yields $\Omega(\kappa)$, the "pseudo" divergence required to get the numerical detonation to be compatible with $D_n(\kappa)$. This 2-part model is implemented in a second-order, 2D, multimaterial, Eule-

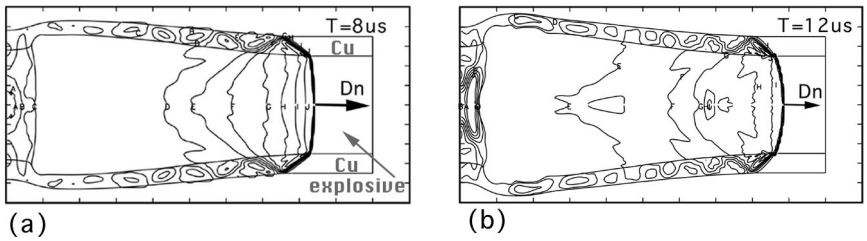

Figure 3. Pressure contours for Mesa calculations of the detonation cylinder test. The detonation wave is moving to the right. Frame (a) shows the results at $t = 8$ μs from the $D_n = D_{CJ}$ model, (b) shows the results for the $D_n(\kappa)$ model at $t = 12$ μs.

rian grid hydrodynamics code at Los Alamos called Mesa (Holian et al. 1989). The results of two calculations of the detonation Cu-cylinder test (one using the standard $D_n = D_{CJ}$ model and the other using DSD) are displayed in Fig. 3. The difference in the timing and wave shapes is striking.

5. Boundary-condition study

A complete theoretical analysis of fully 2D, reactive edge flows is out of reach. Here we present some results obtained using high-resolution numerical simulations. A limited amount of supporting theory is offered to help with the interpretation of these results.

We study a simplified Euler fluid model, and use a polytropic EOS with a large γ to mimic condensed phase explosive, where

$$e = \frac{P}{(\gamma - 1)\rho} - q\lambda \ , \tag{8}$$

with $\gamma = 3$, an initial density $\rho_0 = 2000$ kg/m^3, and a heat of detonation $q = 4 \times 10^6$ m^2/s^2, so that $P_{CJ} = 3.2 \times 10^{10}$ N/m^2 is large. A simplified state-independent rate law is used ($k = 2.51 \times 10^6$ s^{-1})

$$(\dot{\lambda}) = R = k\sqrt{1 - \lambda} \ , \tag{9}$$

for which the 1D steady-state reaction-zone length is 4×10^{-3} m and the particle reaction time is 0.8 μs. The numerical simulations were done using a second-order Godunov code called Caveat (Addessio et al. 1990). The grid size used in the calculations was 2×10^{-4} m in the streamwise direction. Two types of boundary interactions are studied here. For both, the detonation is initially a plane ZND wave whose direction of propagation is colinear with a *flat rigid* wall (i.e., $\omega = 90°$). Problem (1) considers the response of the detonation to a sudden loss of confinement, while the interaction of the detonation with a converging, rigid wedge is studied in problem (2).

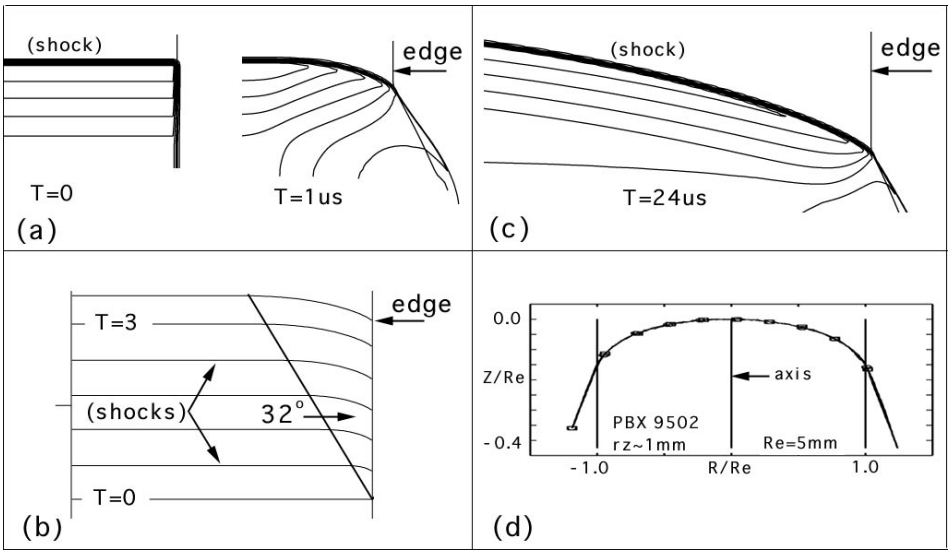

Figure 4. Response of a detonation reaction zone to a sudden loss of confinement. Frames (a), (b), (c), and (d) show the reaction-zone pressure contours, the evolving shock-front shape, late-time pressure contours, and an experimentally measured shock-front shape, respectively.

5.1. Loss of confinement

A collection of the results from problem (1) is shown in Fig. 4. Propagating upwards initially, the detonation loses confinement along its right boundary at $t > 0$. Figure 4a shows strong 2D flow at the edge as evidenced by $P_\xi = O(1)$ and the rapid change in the shock slope (ω changes from 90° to 55°). The Prandtl-Meyer expansion that develops limits the decrease in pressure at the shock which results in a fixed shock-edge angle after a very short transient, as shown in Fig. 4b. The rarefaction moves along the shock at $(\sqrt{C^2 - (D_n - U)^2})_{\eta=0} = 0.7 D_{CJ}$. Figure 4c shows a broadly curved DSD wave at $t = 24$ μs. The value $\omega_c = 55°$, corresponds to a flow that is exactly sonic as measured with respect to the shock-edge intersection point. A discussion of the effect that increasing confinement and changes in ω_{in} have on these results is given elsewhere (Bdzil & Stewart 1986, Aslam et al. 1995). The experimentally measured shock-arrival trace for a $Re = 5$ mm radius detonating cylinder of PBX 9502 is shown in Fig. 4d. The $\omega_c = 45°$, corresponds to the sonic angle for this material. For this explosive, $\eta_r = 1$ mm. Measured on this scale, the shock for this 10-mm diameter explosive is *broadly curved*.

5.2. Converging wedge

A collection of results from problem (2) is shown in Fig. 5. A ZND detonation propagating to the left meets a rigid, converging wedge at $x = 190$ mm ($x = 0$ is at the left). Standard three-shock theory for a CJ detonation predicts Mach reflection for $\omega_{in} \geq 45°$. A simulation of the 50° wedge problem shows regular reflection. The evolving shock and D_n for both a 40° and 20° wedge shown in Fig. 5a display irregular reflection. The pressure contours at $t = 24$ μs shown in Fig. 5b reveal that the irregular reflection grows slowly for the 40° case. Although the structure looks somewhat classical, the reflected wave is clearly dispersed.

The pressure contours at $t = 24$ μs for the 20° wedge reveal a totally nonclassical von Neumann reflection (Colella & Henderson 1990). The leading shock is broadly curved with no evidence of a reflected shock. This is a consequence of the diffraction of the reflected wave by the reaction-zone flow gradient. By contrast, the Mach reflection of an inert shock of comparable strength, shown in Fig. 5d, is classical. Figure 5e shows "Mach" reflection during the collision of two PBX 9502 detonations. These measurements were made at Los Alamos by Larry Hull (Hull 1995). With the progress of time (time advances to the left), the wave-interaction region (the left-most part of each trace) becomes wider and more "rounded."

We present a qualitative theoretical argument to help understand these ob-

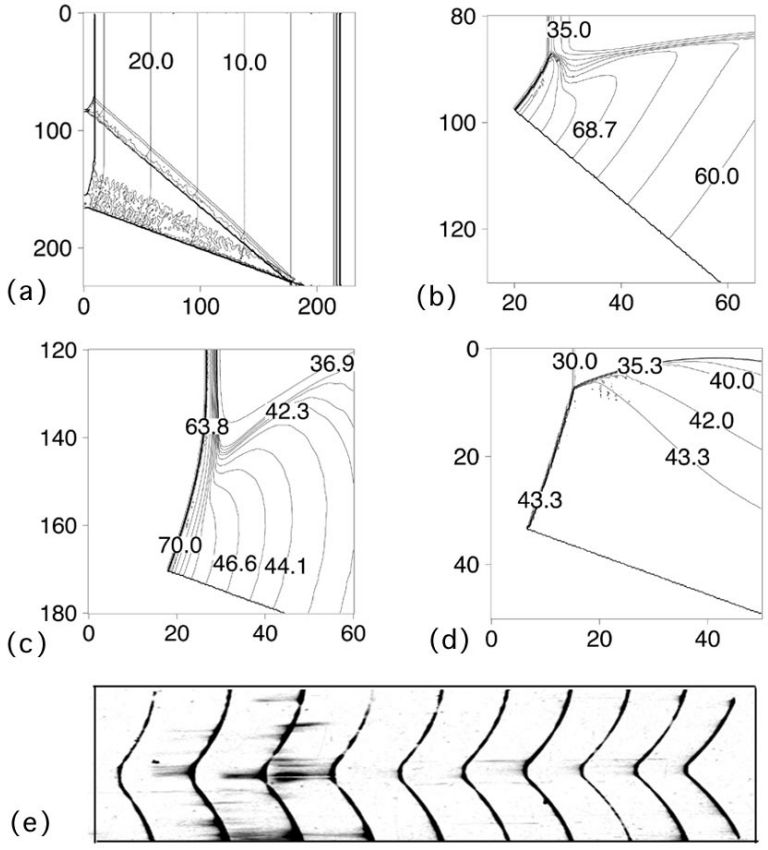

Figure 5. The oblique interaction of a resolved reaction zone detonation with a rigid wedge. Frames (a), (b), (c), (d), and (e) show the evolving lead shocks for a 40° and 20° wedge, pressure profiles at $t = 24$ μs for the 40° and 20° wedge, a strong inert shock over a 20° wedge and the curved "Mach" interaction for PBX 9502, respectively.

servations. Equation (4) is exact along the shock

$$(D_n^2)_t = \frac{(\gamma+1)^2}{3}\left(\frac{(\gamma-1)}{(\gamma+1)}D_n^2\right)(U_\eta)_{\eta=0} + \frac{(\gamma+1)}{(\gamma-1)}\frac{D_{CJ}^2}{6}(R)_{\eta=0} - \frac{4\gamma}{3(\gamma+1)}D_n^3\kappa \ . \tag{10}$$

Differentiating Eq. (10) with respect to ξ, using the shock-compatibility condition, and then transforming the resulting equation to a reference frame moving at acoustic speed along the shock ($\nu = -(\sqrt{C^2-(D_n-U)^2})_{\eta=0}$ with $d\omega \equiv d\xi - \nu dt$), allows us to derive an equation for the amplitude of the leading edge of a weak 2D disturbance moving into a 1D ZND detonation

$$4\tilde{K}_\tau = -\frac{2(\gamma+9)}{3(\gamma+1)}\tilde{K}^2 - \frac{(\gamma+1)}{6(\gamma-1)}(1-\sigma)\tilde{K} + \frac{2(\gamma-3)}{3\sqrt{\gamma^2-1}}\tilde{K}_{\tilde{\omega}} + O((U_{\eta\omega})_{\eta=0}) \ . \tag{11}$$

The variable $\tilde{K} \equiv (\kappa D_{CJ}/k)_{wavehead}$ is the scaled shock curvature, $\tau = kt$

is the scaled time, and σ measures the state dependence of the rate (e.g., $R = k\sqrt{1-\lambda}\exp(\sigma D_n/D_{CJ})$). The strength of the 2D disturbance is $\tilde{K}$, with $|\tilde{K}| \to \infty$ denoting triple-point formation on the shock. Neglecting the $O((U_{\eta\omega})_{\eta=0})$ term in Eq. (11), setting $\gamma = 3$, and solving, one finds that for $\sigma < 1$, $\tilde{K} \to 0$ when $\tilde{K}_{t=0} > -(1-\sigma)/6$ and $\tilde{K} \to -\infty$ otherwise. Thus, sufficiently weak convergence does not lead to triple points. This is what we see in our simulations. Suppressing the reaction-related terms in Eq. (11), one finds that all levels of convergence lead to triple points for inert flows. The DSD boundary conditions derived from this example are: (1) when $\omega_{in} < \omega_s = 35°$, then $\omega_{out} = \omega_{in}$ and (2) when $\omega_{in} > \omega_s = 35°$, then $\omega_{out} = \omega_c = 90°$.

Acknowledgement. We thank Rudy Henninger for Mesa-DSD. John Bdzil was supported by the U.S. Department of Energy. Tariq Aslam and Scott Stewart were supported by the U.S. Air Force, Wright Laboratory, F08630-92-K0057.

References

Bdzil JB, Stewart DS (1989) Modeling two-dimensional detonation with detonation shock dynamics. Phys Fluids A 1:1261–1267.

Aslam TD, Bdzil JB, Stewart DS (1995) Level set methods applied to modeling detonation shock dynamics. Journal of Computational Physics (to appear).

Osher S, Sethian JA (1988) Fronts propagating with curvature-dependent speed: algorithms based on Hamilton-Jacobi formulations. Journal of Computational Physics 79:12–49

Colella P, Henderson LF (1990) The von Neumann paradox for the diffraction of weak shock waves. J Fluid Mech 213:71–94

Bdzil JB (1981) Steady-state two-dimensional detonation. J Fluid Mech 108:195–226

Bdzil JB, Stewart DS (1986) Time-dependent two-dimensional detonation: the interaction of edge rarefactions with finite-length reaction zones. J Fluid Mech 171:1–26

Stewart DS, Aslam TD, Yao J, Bdzil JB (1995) Level-set techniques applied to unsteady detonation propagation. *In*: Modeling in Combustion Science, Springer-Verlag, Berlin (to appear).

Whitham GB (1973) Linear and Nonlinear Waves, Wiley, New York.

Holian KS, Mandell DA, Adams TF, Addessio FL, Baumgardner JR, Mosso SJ (1989) Mesa: A 3-D Computer Code for Armor/Anti-Armor Applications. *In*: Supercomputing World Conference, Oct 17-20, 1989, San Francisco, CA.

Addessio FL, Baumgardner JR, Dukowicz JK, Johnson NL, Kashiwa BA, Rauenzahn RM (1990) Caveat: A Computer Code for Fluid Dynamics with Large Distortions and Internal Slip. Los Alamos Report, LA-10613.

Hull LM (1995), Los Alamos National Laboratory, Private communication.